Korean J. Chem. Eng., **26**(1), 64-71 (2009)

Separation and characterization of bitumen from Athabasca oil sand

Songhun Yoon*, Sharad Durgashanker Bhatt*, Wonkyu Lee, Heung Yeoun Lee**, Soon Yong Jeong*, Jin-Ook Baeg*, and Chul Wee Lee*,†**

*Advanced Chemical Technology Division, Korea Research Institute of Chemical Technology (KRICT), Daejeon 305-600, Korea
**Korea National Oil Corporation, Petroleum Technology Institute, Anyang 431-711, Korea

(*Received 7 July 2008 • accepted 24 July 2008*)

Abstract−Separation and chemical analysis was investigated using bitumen samples from Athabasca oil sand in Alberta. Fractionation according to solubility and polarity has been used to separate bitumen into its fractions. The solvent de-asphaltening was performed by n-pentane solvent (solubility fractionation), and the polarity fractionation using Fuller's earth allows maltene to separate into SARA components (saturates, aromatics, resins and asphaltenes). The SARA components are analyzed comprehensively using elemental analysis (EA), Fourier-transformed infrared (FT-IR), ultraviolet-visible spectroscopy (UV-vis), high performance chromatography (HPLC) and thermogravimetric analysis (TGA). EA (C, H, N, S), heavy metals (Ni, V) concentrations, FT-IR and UV-vis tests provided the explanation of chemical composition. From IR spectra, maltene and saturates/aromatics (sat/aro) contained more aliphatic compounds than resin or asphaltene. Also, IR spectrum of sat/aro was similar to crude oil and VGO (vacuum gas oil). Different UV signal data clearly indicates the contribution of aromatic constituents in the fractions. Using optimized analysis conditions of HPLC, we successfully separated the peaks for bitumen and its fractions. The characteristic peak pattern of SARA (saturates, aromatics, resins, asphaltenes) fractions was observed, and also the peak pattern of sat/aro was similar to that of crude oil and VGO. However, TGA results revealed that thermal behavior for sat/aro was similar to that of crude oil but different from that of VGO. Also, from the comparison between decomposition temperature of TGA and boiling point, their correspondence was found.

Key words: Oil Sand, Separation, Bitumen, Heavy Oil, Spectroscopy

INTRODUCTION

Petroleum products play an important role in economic development of any nation [1-3]. The growth in energy consumption is connected to the growth in the economy of any country; however, the energy demand of the world is increasing while conventional oil reserves are declining. The shortage of oil of known petroleum reserves will make less attended energy resources more attractive. The most feasible way to meet this growing demand is by utilizing such sources as bitumen, which is a huge potential resource to fulfill petroleum requirements of processes significantly [4-7]. Bitumen is a mixture of organic liquids that is viscous, black and sticky. It is a complex mixture of high boiling point range of compounds and molecules with a relatively low hydrogen-to-carbon ratio. It has an abundance of chemical impurities. Many countries in the world have large deposits of bituminous sands, commonly referred to as oil sands, including America and Russia. However, the largest deposits of the world oil sand occur in Canada and Venezuela. The Alberta deposits contain about 85% of the world's total bitumen reserves and are economically recoverable for conversion into synthetic crude oil. Bitumen becomes gradually more important as a refinery feedstock. In order to optimize quality, more information on its molecular chemistry is required. Much of this attempt has been directed at the whole bitumen and limited information is available on the characteristics of narrow fractions of bitumen.

Solvent extraction and fractionation with n-pentane provides the information regarding the details of the individual characterization and reactivity studies. Various methods are developed to characterize the compositional determination of fractions of bitumen [8-10]. Wik et al. have investigated that the variability in ore composition and process parameters is known to affect bitumen recovery from natural oil sands [11]. A mechanism for the hot water extraction process is proposed [12]. Vacuum distillation and chromatography separation technique for bitumen was reported [13]. Zhao et al. [14] have led the development of a super-critical extraction technique for hydrocarbon fractionation to compare the chemical and physical properties of fractions of residua from Venezuelan heavy oil, a Saudi Arabian light crude and a Chinese Daqing conventional crude. Yu et al. have performed bitumen fractionation with supercritical CO_2 [15]. Rapid and selective high performance liquid chromatography method using a column-switching technique has been developed to analyze industrial products such as oil and bitumen [16]. Wood et al. have fractionated bitumen by high performance liquid chromatography [17]. It is possible to convert bitumen to high quality oil as a premium replacement for conventionally produced oil.

The objective of this study was to investigate physico-chemical characteristics of narrow-cut fractions and to find correlation with conventional petroleum hydrocarbon. The solvent deasphaltening is performed by using n-pentane solvent (solubility fractionation) and the polarity fractionation using Fuller's earth allows maltene to separate into SARA components (saturates aromatics, resins and asphaltenes). The SARA components are analyzed comprehensively by using elemental analysis (EA), Fourier-transformed infrared (FT-

---

[†] To whom correspondence should be addressed.
E-mail: chulwee@krict.re.kr

IR), ultraviolet-visible spectroscopy (UV-vis), high performance chromatography (HPLC) and thermogravimetric analysis (TGA).

EXPERIMENTAL

1. Materials

Bitumen from the Athabasca oil sands was used in this study. As reference hydrocarbon to compare with bitumen and its fractions, crude oil and its distillation fractions such as VGO (vacuum gas oil), kerosene were used.

2. Solvents and Sample Preparation

n-Pentane, toluene and THF, and other chemicals from Sigma-Aldrich were used for sample solution preparation.

3. Bitumen and its Fractions

Basically, fractionations were carried out according to the literature and the main four different fractions were obtained, being assigned as asphaltene, maltene, saturate aromatics, and resins. Bitumen was weighed and mixed with n-pentane and toluene in a proportion of 12 g : 480 ml : 24 ml for the separation of soluble and insoluble fractions. n-pentane insoluble fraction, namely, asphaltene was separated on filter paper. The n-pentane soluble fraction, namely maltene, was subjected to fuller's earth for extraction of saturate aromatics and resins. Fuller's earth and adsorbed resin were separated by filtering and soluble fraction was saturate aromatics. Standard materials such as naphtha, kerosene, VGO were analyzed simultaneously for better understanding of the fractions from bitumen for comparison.

4. Elemental Analysis

Carbon, hydrogen, nitrogen, sulfur and oxygen content were determined by using a CHNSO Fisons EA-1108 Elemental Analyzer.

5. FT-IR

IR spectra of different fractions of bitumen were recorded on a Bruker equinox 55 spectrophotometer in the region of 4,000-400 cm^{-1} using KBr pellets.

6. UV-VIS

Spectra were recorded on Shimadzu UV-2100 in the range of 240-600 nm.

7. HPLC

The HPLC analysis was performed using Younglin instruments, which consisted of a gradient pump, column heater module, binary pump and DAD, the MS detector, and a fluorescence-detector. The Luna RP18 (Phenomenex-Torrance CA) column, 250 mm×4.6 mm (5 μm), was used. Analytical conditions included a mobile phase of 0.9 ml/min of THF/H_2O 7/3. The UV absorbance was measured at λ=254 nm at room temperature.

8. TGA

Thermo-gravimetric experiments were recorded on a TA instrument TGA Q500 operating under nitrogen with a flow rate of 100 ml min^{-1} through the furnace in the following conditions: samples weight about 10 mg, varying heating rates of 10 $^{\circ}C$ min^{-1}, temperature range of 100-1,000 $^{\circ}C$.

RESULTS AND DISCUSSION

Bitumen quality varies from place to place; hence it is required to know the quality of bitumen before processing to upgrade. The quality of bitumen depends on the hydrocarbon constituents and their concentrations; hence detailed structural and compositional study of bitumen is required to utilize it properly.

1. Extraction of Bitumen

It is well known that light paraffins provide much higher extraction yields during fractionation of heavy hydrocarbons [18]. If suitable solvent and operating parameters are selected, extraction and fractionation will provide high extraction yields and enough amounts of samples for reactivity and conversion studies; thus *n*-pentane is the extractant of choice for this study.

Athabasca bitumen sample was first extracted with n-pentane and the obtained extract was treated by fullers' earth. This fractionation can be separated bitumen into the SARA components (saturates, aromatics, resins and asphaltenes) for analysis. The analysis data of the SARA components are presented in Table 1, where the comparison of chemical properties of Athabsca bitumen and its fractions with other bituminous samples is shown. The fractionation distribution shows that asphaltene, maltene, saturate aromatics and resin content of Athabsca bitumen are 15.59, 84.41, 67.97 and 16.44%, respectively. These fractions can vary with place and geographical conditions, including depth. The result indicates that Athabasca bitumen is quite rich in trace elements such as vanadium and nickel, which are known to be toxic metals. Because these metals can poison the catalyst used in the upgrading processes such as hydrocracking, it is desirable to remove them before the upgrading process. Furthermore, sulfur content in Athabsca bitumen is higher than in other

Table 1. Comparison of chemical properties of Athabasca bitumen with other residues from various sources [20]

Contain	Daqing	Shengli	Saudi medium	Iranian heavy	Oman	Athabasca bitumen
Density at 20 $^{\circ}C$ (g/cm)	0.9392	0.9724	1.0258	1.0222	0.9637	0.8973
H/C (atomic)	1.79	1.58	1.51	1.44	1.60	1.50
S (wt%)	0.15	3.01	4.79	3.11	1.68	4.78
N (wt%)	0.44	0.95	0.53	0.62	0.45	1.63
Ni (ppm)	7.60	55.70	36.70	90.00	18.00	68.50
V (ppm)	0.1	3.3	147.4	205.8	21.8	174.00
Asphaltenes (wt%)	0.00	2.20	9.30	10.80	2.00	15.59
Maltene (wt%)	0.00	97.8	89.60	89.10	98.10	84.41
Saturate aromatics (wt%)	74.6	46.7	55.90	59.20	66.90	67.97
Resin (wt%)	25.4	51.1	33.7	29.9	31.20	16.44
Reference	20	20	20	20	20	This work

Table 2. Elemental analysis of Athabasca bitumen and its fractions

	Bitumen	Asphaltene	Maltene	Saturate aromatics	Resin	Crude oil	VGO
C (wt%)	82.84	80.71	84.78	85.04	81.06	77.71	83.75
H (wt%)	10.40	7.95	10.85	11.59	10.04	11.00	12.16
N (wt%)	1.63	0.99	1.32	1.18	0.86	0.41	1.13
S (wt%)	4.78	8.35	3.65	3.96	5.52	2.74	2.79
O (wt%)	1.81	2.07	1.31	0.98	3.09	0.53	0.56
H/C (atomic)	1.50	1.18	1.53	1.63	1.48	1.70	1.74
Fraction (wt%)	-	15.59	84.41	67.97	16.44	-	-
Fe ppm	16.80	n.a.	n.a.	n.a.	n.a.	n.a.	n.a.

n.a.=not analyzed

bitumens.

In Table 2, the result of elemental analysis for Athabasca bitumen and its fractions is presented. As shown, H/C atomic ratio is highest in saturates/aromatics (sat/aro) fraction among Athabasca bitumen fractions, while asphaltenes have the lowest H/C atomic ratio due to variation in hydrocarbon contents. The large H/C atomic ratio means low density, low content of aromatic hydrocarbons and high cracking reactivity, resulting in high yields of light hydrocarbons and low yield of coke. Also, polar species such as S and O were higher for asphaltene and resin than sat/aro. The amount of asphaltene extract from bitumen depends on the type of solvent, dilution ratio, contact time, and temperature [19]. The elemental composition of asphaltene showed a ratio of H/C=1.18, which matches with the reported data of various sources [19]. For comparison, EA data of crude oil and its distillation fraction (vacuum gas oil: VGO) are listed in Table 2. Unfortunately, it was impossible to obtain EA data of kerosene due to its high volatility during heating. In Table 2, the H/C mole ratio is very high for crude oil and VGO.

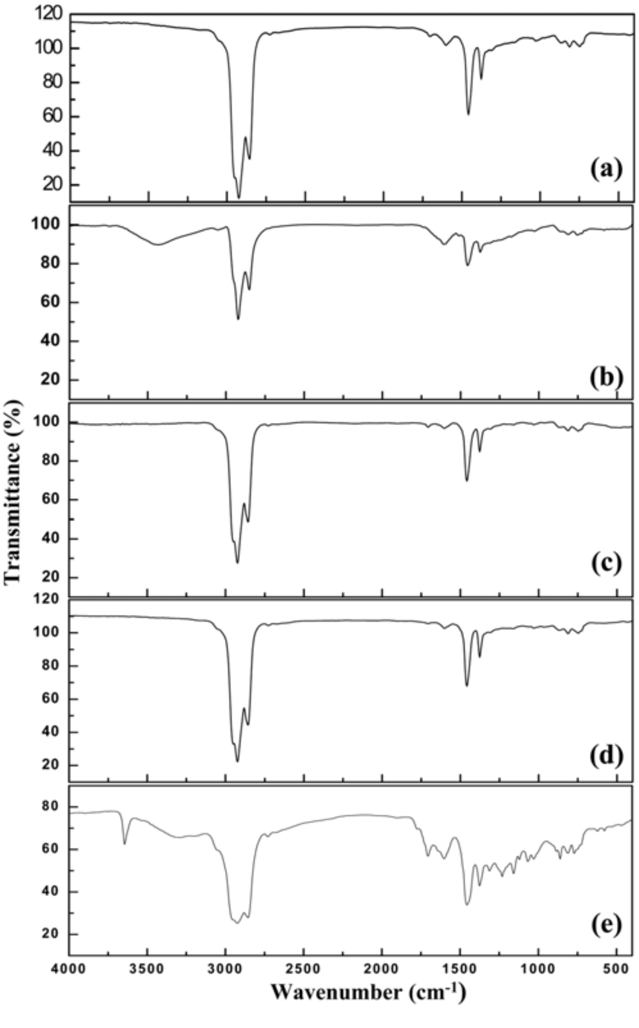

Fig. 1. FT-IR spectra of (a): bitumen, (b): asphaltene, (c): maltene, (d): saturate/aromatic and (e): resin.

2. FT-IR Spectra

After fractionation from bitumen, all the fractions including bitumen were characterized by FT-IR spectroscopy [17,20-22]. IR analysis can reveal the information about functionality and constituents of hydrocarbons. In Fig. 1, IR spectra of bitumen and its four fractions are shown with an expansion of 4,000-400 cm^{-1} region.

Strong absorbances are observed at 2,924, 2,855, 1,458 and 1,376 cm^{-1} corresponding to the distribution of aliphatic hydrogen between $-CH_2$ and $-CH_3$ structures caused by C-H stretching in $-CH_3$ and $-CH_2$ for bitumen. These bands are observed common in all the fractions of bitumen with minor shifting as shown in Fig. 1. The absorbance for the $-CH_3$ group at about 2,924 cm^{-1} is common in all fractions. This may be due to $-CH_3$ substituents on aromatics rings in all fractions. Bitumen and all the fractions show the absorbances at about 2,855, 1,601, 1,458 and 1,376 cm^{-1} and can be attributed to C-H stretching in $-CH_3$, C=C stretching, C-H deformation in $-CH_2$ and $-CH_3$, respectively. Presence of shoulders at 1,601, 1,029, 812 and 747 cm^{-1} is observed in bitumen and with little shifting in all the fractions of bitumen, which may be due to $-CH_3$ substituents on aromatics rings in all fractions. The peak in the region between 1,000 cm^{-1} and 1,300 cm^{-1} is attributed to sulfur structure. The peak around 1,029 cm^{-1} could be due to -C-O vibration in alkyl-aryl ether and -S=O stretching. The spectral band at 747 cm^{-1} is attributed to the four adjacent hydrogen atoms on the aromatic ring, and the band at 812 cm^{-1} is due to two or three adjacent hydrogen atoms.

IR spectra of asphaltene, as shown in Fig. 1(b), have peaks together at 810 cm^{-1} and 755 cm^{-1} with a tail at 3,052 cm^{-1} which indicates the presence of aromatic rings. Asphaltene showed different bands at 3,434 cm^{-1} corresponding to O-H and N-H stretching in multiple hydrogen bonded compounds. Also, the relative intensity of bands relevant to aliphatic hydrogene at 2,924, 2,855, 1,458 and 1,376 cm^{-1} was decreased when compared with those of maltene (Fig. 1(c)). It is observed that there is no big difference between maltene and saturate/aromatics in the IR spectra, as shown in Fig. 1(c) and (d), respectively. This result indicates that the main fraction of maltene was sat/aro. Fig. 1(e) shows that the remarkable IR spectra of resin at 3,285 cm^{-1} is due to O-H and N-H functional groups, which are related to hydrogen bonding. This may be due to presence of polar groups. According to the literature, the boiling point of resin was higher than that of sat/aro, which can be attributable to a large amount of polar groups in resin. This will be discussed with the comparison of HPLC result later. Resin fraction showed additional bands at 3,644, 3,285 and 2,729 cm^{-1} for O-H stretching in non H-bonded alcohols, O-H and N-H stretching in multiple H bonded compounds and C-H stretching at the bridge head position in naphthenes, respectively. The peak around 1,706 cm^{-1} of maltene and resin indicates the presence of carbonyl group, which resonate in 1,720-1,680 cm^{-1} range, for both non hydrogen bonded and hydrogen bonded acids, and amide carbonyl, which resonate in the 1,700-1,650 cm^{-1} region. Also, a strong band at 3,644 cm^{-1} is attributed to phenolic OH stretching for non-bonded resonate at 3,610 cm^{-1}. Hence, the change of IR spectrum according SARA components indicates that the amount of aliphatic compound and functional group is varied during fractionation.

In Fig. 2, IR spectra of reference hydrocarbons such as crude oil, VGO, Kerosene are presented. All of three spectra are almost the same and very similar to that of saturate/aromatic in Fig. 1(d), reflecting that the major contents of these hydrocarbons are aliphatic hydrocarbon.

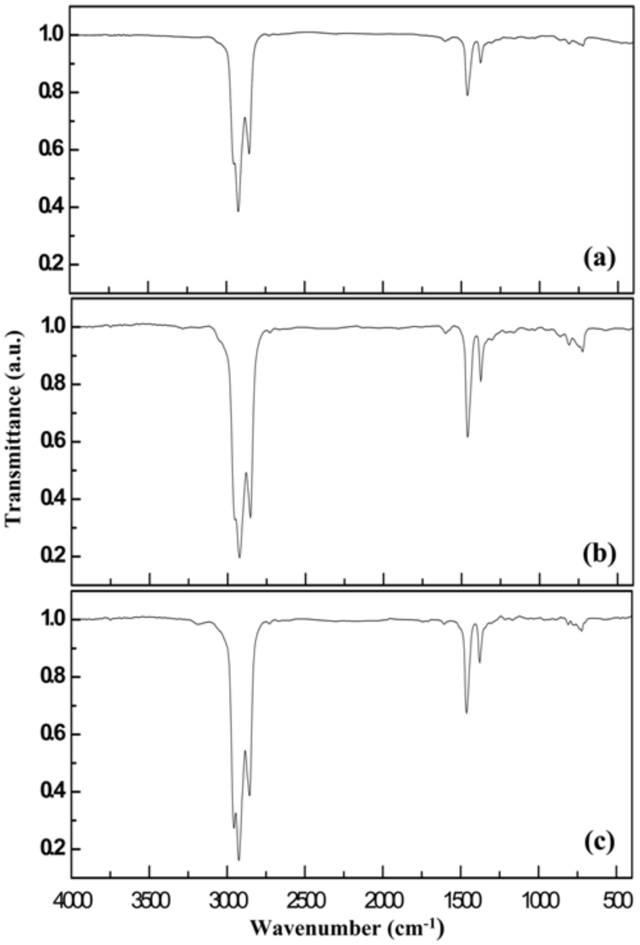

Fig. 2. FT-IR spectra of (a): crude oil, (b): vacuum resin and (c): kerosene.

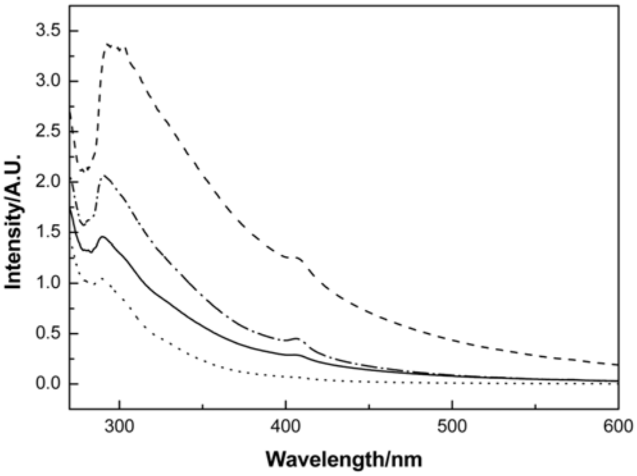

Fig. 3. UV-Vis spectra of bitumen (solid line), asphaltene (dashed line), resin (dash-to-dotted line) and saturate/aromatic (dotted line).

3. UV-Visible Spectra

The UV instrument was set to collect UV signal data in the range of 240-600 nm as shown in Fig. . This UV range is selected due to its particular sensitivity to the fractions with high contents of aromatic molecules. According to the literature [23], it is reported that the onset wavelength of absorption peak of benzene, naphthal, antharcene, tetracene and pentacene exists near 270, 320, 380, 470 and 580 nm, respectively. As seen in Fig. 3, thereby all the spectra show major absorption bands in the range of 270-400 nm, indicating that the constituents containing 2 or 3 benzene-fused rings are dominant for every fraction. Another feature observed in Fig. 3 is that the relative intensity of peaks is in the order of asphaltene>resin> saturate aromatics. This illustrates that aromaticity of fractions increases in the same order. Note that all the fractions show a peak at 410 nm, which is attributable to the presence of VO^{2+} complex [24]. The higher intensity of this peak in asphaltene demonstrates the asphaltene contain higher amount of vanadium impurity. This result is in agreement with reported by Baginska [25].

4. HPLC

Fig. 4 shows the HPLC of bitumen and its three different fractions, namely maltene, sat/aro and resin obtained from solvent separation. Luna RP18 (Phenomenex-Torrance CA) column (5 μm) was used as HPLC column. This column is highly sensitive to the hydrophobicity of analyzed species and recommended to be suitable to separate PAH (poly aromatic hydrocarbon). During separation of PAH, the retention time (RT) was proportional to molecular weight, increasing hydrophobicity. As a preliminary experiment, peak positions of benzene and anthracene were 4.78 and 5.14 min, respectively, under the analysis condition in this work. It is observed that the composition of eluate THF/H_2O (ratio of 7/3) provides high resolution for the fractions of bitumen at a reasonable retention time within 25 min. According to the literature [17], it has been reported that the peak separation of bitumen and its fractions was difficult

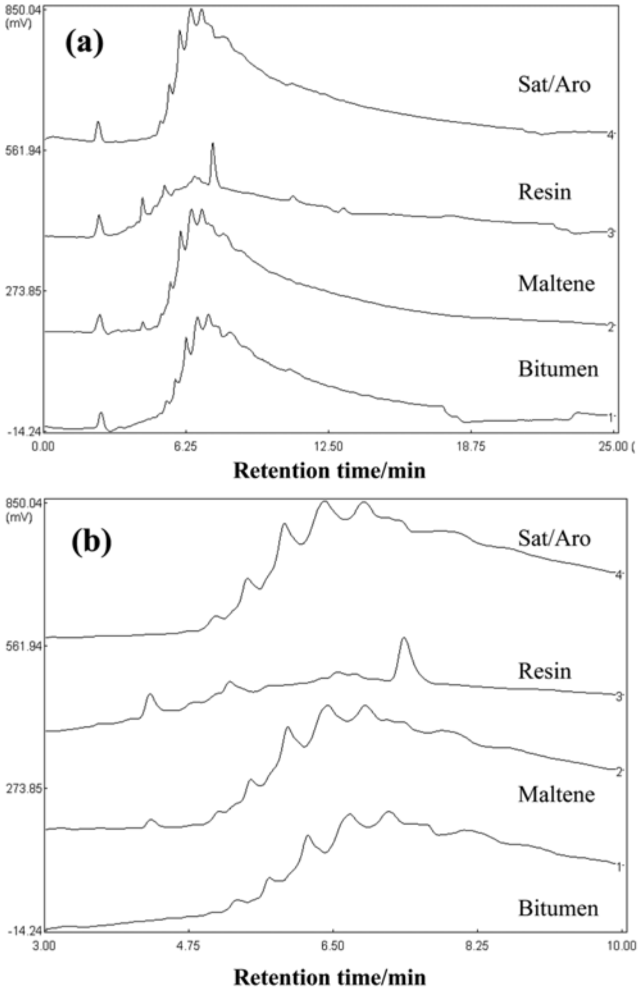

Fig. 4. HPLC results of bitumen and its three different fractions. Their names are inserted for easy comparison. (a): Full chromatogram from 0 to 25 min, (b): magnified region from 3 to 10 min.

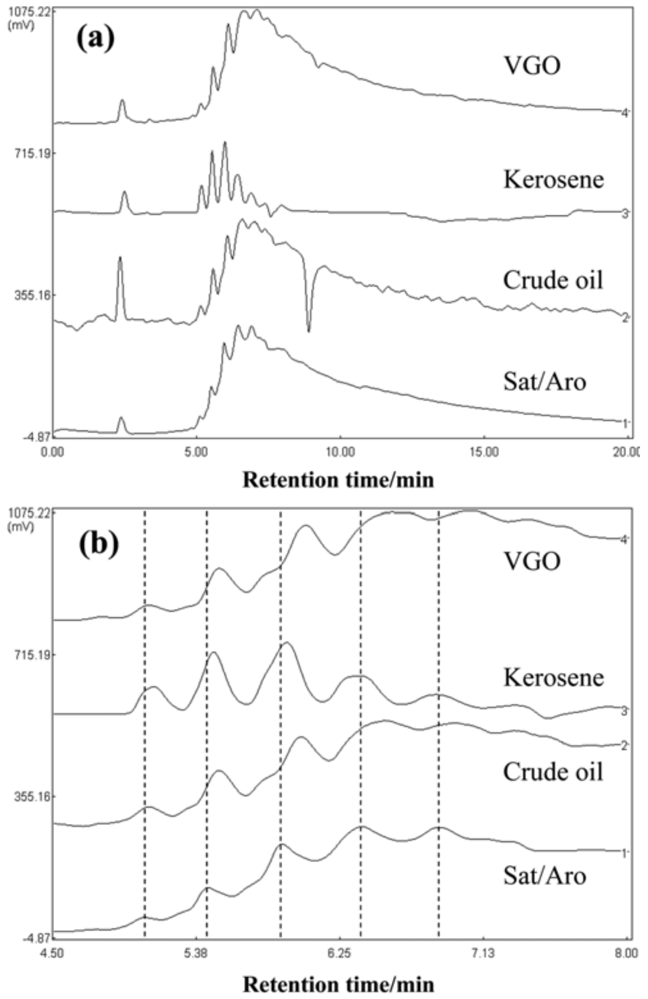

Fig. 5. HPLC results of saturate/aromatic, crude oil, kerosene and VGO, of which names. are inserted for easy comparison. (a): Full chromatogram from 0 to 20 min, (b): magnified region from 4.5 to 8 min.

because the peak intensity and position were highly sensitive to the selection of column, eluate ratio and sampling amount. In our experiment, however, the optimal HPLC analysis condition of bitumen and its fractions was successfully found.

As shown in Fig. 4, all the chromatograms are started after the peak at 2.5 min of retention time (RT), which is relevant to elution of THF used as a solvent in samples. After the retention time at 25 min, no peaks appeared, reflecting an end of collection of hydrocarbons using the HPLC column. It was observed that the peak's intensity was increased in maltene fraction compared to bitumen, which can be due to the removal of asphaltene fraction with more polar and higher molecular weight constituents from bitumen. From a preliminary experiment, no noticeable peaks were observed for asphaltene, and this may be due to low solubility of asphaltene in eluant composed of THF/water (7/3). Along this line, it was reasonable that the peak intensity of maltene also decreased because it contains 15.59 wt% asphaltene content. For clear comparison, the range from 3 to 10 min was magnified in Fig. 4(b). Different peak position and shape were observed clearly from maltene to resin and sat/aro. Peaks from 4 to 5 min became more apparent from maltene to resin, which corresponds to low molecular weight, and polar species contained in resin. Also, the peaks become broader for resin, indicating larger content of more hydrophobic species in resin (larger population of high molecular weight and high aromaticity species). From maltene to sat/aro, peak shape and position were very similar.

To investigate the peak pattern in sat/aro, HPLC analysis of crude oil, kerosene and VGO was performed and compared with that of sat/aro as shown in Fig. 5. Fig. 5(a) shows the peak pattern of sat/aro was almost similar to VGO and crude oil. Main difference was observed in the larger peak area of sat/aro after a retention time of 12 min, demonstrating higher concentration of high molecular weight in sat/aro. Abrupt decrease of intensity near 8 min was observed in crude oil. The chromatogram from 4.5 to 8 min was magnified in Fig. 5(b) for better comparison. Interestingly, the characteristic 5 peaks from 5 to 7 min were observed for every sample. For kerosene, the peak intensity becomes smaller with increasing of RT, indicating smaller population of species with higher molecular weight in kerosene. The peak shape and pattern of VGO and crude oil were almost similar to sat/aro, although the peak positions were slightly different for the three samples. This reflects that the constituents of the three samples have similar molecular structure and weight. This result coincided with the IR spectra of Fig. 1(d) and 2. However, a decrease of peak intensity was observed for VGO after 7 min, in contrast to the case of sat/aro and crude oil (see Fig. 5(a) for comparison). This illustrates that higher molecular weight species exist in the latter two cases.

5. TGA

TGA method has been employed to compare the thermal behavior of the bitumen and its fractions in nitrogen environment. The study of TGA of bitumen and its fractions is extremely complicated because of the presence of many complex constituents.

Conventional hydrocarbon can be fractionated according to boiling point cut in the distillation method as follows:

Naphtha: bp<177 °C (region 1: R1)
Kerosene: 177 °C<bp<343 °C (region 2: R2)
Gas oil: 343 °C<bp<525 °C (region 3: R3)
Vacuum residue (VR): 525 °C<bp<525 °C (region 4: R4)
Cokes: bp>700 °C (region 5: R5)

Similar to the classification by boiling point, the TGA curve was separated into five regions, which were indicated in the parentheses. Fig. 6 shows the TGA of bitumen and its fractions, showing different thermal decomposition behavior. It is assumed that the weight loss observed in the bitumen and its fractions represents the thermal decomposition [26,27]. The differences indicated in the thermogravimetric characteristic values of the samples, especially in terms of weight loss, are due to the different constituents of each fraction. The weight loss is decreased in the order of saturate aromatics>maltene>bitumen>resin. Weight loss is about 80% for resin, whereas it is 95% for saturate aromatics up to 500 °C. The weight loss after 800 °C is almost negligible and carbon-rich residue (coke) is formed. Similar observation has been reported [28]. The asphaltene has maximum carbon residue and other non-volatile materials left after high temperature combustion, whereas saturate aromatic has a minimum. In Fig. 6(a), the amount of R1, R2, R3, R4 and R5 content shows a definite trend. The R1 content is more in maltene than that of sat/aro and resin fractions. However, maltene has major R2 content. The sat/aro fraction has more R2 content compared to maltene and resin fractions. The resin fraction has greater R3 content than others. The R4 content is greater in the resin fraction. R5 content also increases in the order resin>maltene>sat/aro fractions. Thus, R2 is the major fraction for maltene and sat/aro fraction and R3 is dominant for resin fraction.

To identify the physical meaning of regional analysis of bitumen and its fractions, TGA was performed for crude oil, VGO and

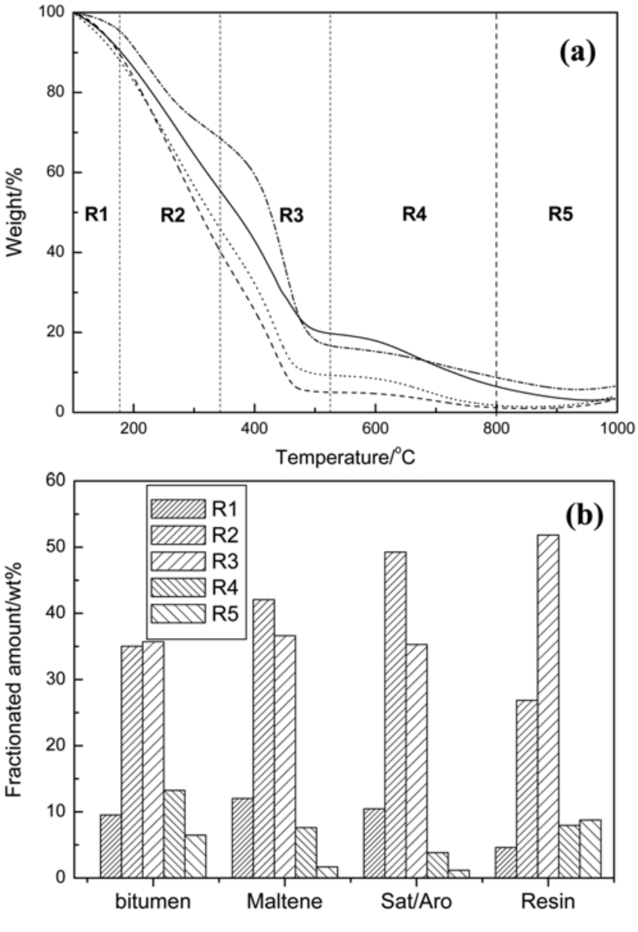

Fig. 6. (a): TGA results of bitumen (solid line), resin (dash-to-dotted line), maltene (dotted line) and saturate/aromatic (dashed line), (b): Comparison of region content in TGA experiments for bitumen and its three fractions.

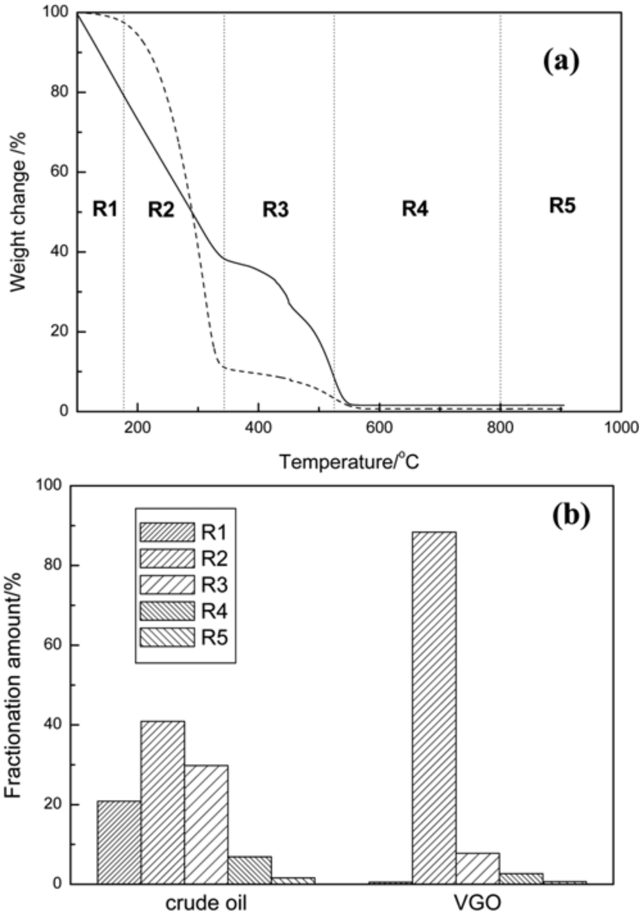

Fig. 7. (a): TGA results of crude oil (solid line), and VGO (dashed line), (b): Comparison of region content in TGA experiments for crude oil and VGO.

kerosene. As shown in Fig. 7(a), trace amount of residue was left after 550 °C, reflecting the presence of typical conventional hydrocarbon materials in the samples. Kerosene was decomposed completely before 150 °C (not shown here). Regional analysis was plotted as shown in Fig. 7(b) based on Fig. 7(a). It was observed that the distribution trend from R1 to R5 of crude oil is similar to that of sat/aro as shown in Fig. 6(b) and Fig. 7(b). Slight difference was observed between these two species, where R2 and R3 contents are higher in sat/aro than crude oil, and R1 content is higher in crude oil than sat/aro. Although there was slight difference in HPLC result of VGO and that of crude oil and sat/aro, TGA curves were very different. Probably, this may be due to the higher polarity of sat/aro (higher amount of S and O) and high aromaticity (low H/C ratio).

Considering the temperature cut for R2 (177 to 343 °C) and R3 (343 to 525 °C), R2 and R3 region should be dominant for kerosene and VGO, respectively, if thermal decomposition temperature in TGA is exactly the same as the boiling point in the distillation process. However, kerosene (177 °C<bp<343 °C), VGO (343 °C<bp<525 °C) had dominant contents of R1 and R2 with minor content of R3, respectively. This difference between boiling point and decomposition temperature can be elucidated as follows. In the standard distillation procedure for bitumen, the used sample volume (ca. 500 mL) is so much larger than that used in TGA (a few mg). So thermal decomposition reaction during the latter experiment can be rapid, which can give rise to a difference between decomposition temperature of TGA and boiling point. Furthermore, as a normal distillation method needs a large amount of bitumen for each experiment, which is complicated to use and requires expensive apparatus, TGA can be a suitable alternative method for analysis of thermal behavior of a small amount of hydrocarbon sample. The correlation can be established between distillation method and TGA analysis for kerosene and VGO as follows.

Naphtha, kerosene≡R1 region
VGO≡R2 region
VR and cokes≡R3~R5

According to the above correspondence, VR wt% of bitumen, maltene, sat/aro, resin, crude oil and VGO were estimated as 55.45, 45.91, 40.32, 68.54, 38.30 and 11.1, respectively. The calculated value of VR of bitumen is quite similar to that reported by the literature (52 wt%) [8]. It is observed very clearly that VR contents of sat/aro and crude oil are similar, which coincides with IR, HPLC results.

CONCLUSIONS

Based on the results presented in this study, the following conclusions can be drawn. The composition of bitumen of Athabasca oil sand was different from other bitumens. The fractionation distribution of Athabsca bitumen shows that contents of asphaltene, maltene, saturate aromatics and resin are 15.59, 84.41, 67.97 and 16.44%, respectively. IR spectra of maltene and sat/aro revealed that they contained more aliphatic compounds than resin or asphaltene. Also, the IR spectrum of sat/aro was similar to crude oil and VGO. Different UV signal data clearly indicates the contribution of aromatic constituents in the fractions. Using optimized conditions of HPLC, we successfully separated the peaks for bitumen and its fractions. We observed the change of characteristic peak pattern of fractions and the peak pattern of sat/aro, which was similar to that of crude oil and VGO, respectively. TGA method was used to compare the thermal behavior of the bitumen and its fractions showing different thermal decompositions for each fraction. A correspondence between decomposition temperature of TGA and boiling point during distillation was also observed.

ACKNOWLEDGMENTS

This work was supported by the Ministry of Knowledge and Economy, Korea National Oil Co. of Republic of Korea. The authors thank SK Energy Co. for providing oil sand sample.

REFERENCES

1. J. Gowdy and R. Juliá, *Energy*, **32**, 1448 (2007).
2. J. Parikh, P. Purohit and P. Maitra, *Energy*, **32**, 1825 (2007).
3. A. D. Sagar, *Energy Policy*, **33**, 1367 (2005).
4. B. Söderbergh, F. Robelius and K. Aleklett, *Energy Policy*, **35**, 1931 (2007).
5. S. Zhao, L. S. Kotlyar, J. R. Woods, B. D. Sparks, K. Hardacre and K. H. Chung, *Fuel*, **80**, 1155 (2001).
6. D. Ferdous, A. K. Dalai and J. Adjaye, *Fuel*, **85**, 1286 (2006).
7. J. Chang, Y. Fu, Y. Shibata, M. Yoshimoto, K. Fujimoto and N. Tsubaki, *Fuel*, **84**, 1661 (2005).
8. S. Zhao, B. D. Sparks, L. S. Kotlyar and K. H. Chung, *Catalysis Today*, **125**, 122 (2007).
9. N. H. G. Rahmani, T. Dabros and J. H. Masliyah, *Journal of Colloid and Interface Science*, **285**, 599 (2005).
10. S. Zhao, Z. Xu, C. Xu, K. H. Chung and R. Wang, *Fuel*, **84**, 635 (2005).
11. S. Wik, B. D. Sparks, S. Ng, Y. Tu, Z. Li, K. H. Chung and L. S. Kotlyar, *Fuel*, **87**, 1394 (2008).
12. O. Dai and K. H. Chung, *Fuel*, **75**, 220 (1996).
13. E. Furimsky and P. J. Champagne, *Fuel Processing Technology*, **6**, 269 (1982).
14. S. Zhao, L. S. Kotlyar, J. R. Woods, B. D. Sparks, J. Gao, J. Kung and K. H. Chung, *Fuel*, **81**, 737 (2002).
15. J. M. Yu, S. H. Huang and M. Radosz, *Fluid Phase Equilibria*, **93**, 353 (1994).
16. C. Champmartin, P. Simon, P. Delsaut, M. Dorotte and B. Bianchi, *Journal of Chromatography A*, **1142**, 164 (2007).
17. J. R. Woods, J. Kung, G. Pleizier, L. S. Kotlyar, B. D. Sparks, J. Adjaye and K. H. Chung, *Fuel*, **83**, 1907 (2004).
18. T. P. Shi, Y. X. Hu, Z. M. Xu, T. Su and R. A. Wang, *Ind. Eng. Chem. Res.*, **36**, 3988 (1997).
19. H. Alboudwarej, J. Beck, W. Y. Svrcek, H. W. Yarranton and K. Akbarzadeh, *Energy & Fuels*, **16**, 462 (2002).
20. S. Zhao, Z. Xu, C. Xu, K. H. Chung and R. Wang, *Fuel*, **84**, 635 (2005).
21. C. J. Pouchert, *The Aldrich library of infrared spectra*, 2nd ed., Aldrich Chemical Company Inc., Wisconsin (1975).
22. R. J. Keller, *The Sigma library of FTIR spectra*, Sigma Chemical Company St. Louis, 1st ed, Missouri (1986).
23. O. Abbas, C. Rébufa, N. Dupuy, A. Permanyer, J. Kister and D. A. Azevedo, *Fuel*, **85**, 2653 (2006).

24. I. N. Evdokimov, N. Y. Eliseev and B. R. Akhmetov, *J. Petroleum Science and Engineering*, **37**, 135 (2003).
25. K. Baginska and I. Gawel, *Fuel Processing Technology*, **85**, 1453 (2004).
26. K. C. Khulbe, R. S. Manna, A. M. Lamarche, G. Lamarche and J. A. MacPhee, *Fuel Processing Technology*, **35**, 303 (1993).
27. K. C. Khulbe, R. S. Mann, A. M. Lamarche, G. Lamarche and J. A. MacPhee, *Fuel Processing Technology*, **41**, 1 (1994).
28. M. Benbouzid and S. Hafsi, *Fuel*, **87**, 1585 (2008).